Design of a Dual-Tone Controller for Lissajous-based Scanning of Fast Steering Mirrors

Ernst Csencsics[1,2], Rudolf Saathof[2] and Georg Schitter[1,2]

***Abstract*— Fast steering mirrors (FMSs) are used in various applications like optical scanning of surfaces, feature detection or beam steering for optical communication systems. This paper introduces Lissajous scan trajectories to improve the tracking performance of a commercial FSM scanning system. The design of a dual tone (DT) feedback controller is presented that is tailored to this type of trajectory and the low-stiffness properties of electromagnetically actuated systems. It is shown that the controller can be used to eliminate periodic errors resulting from remaining cross-talk between the system axes. The DT controller significantly improves the tracking performance as compared to conventional wide bandwidth (WBW) control of the FSM. Applying the tailored controller with Lissajous trajectories reduces the RMS tracking error to 0.77%, as compared to more than 9.1% for the conventional raster scan with a WBW controller. The peak error is reduced from 16% for the raster scan to 1.1% for the Lissajous scan.**

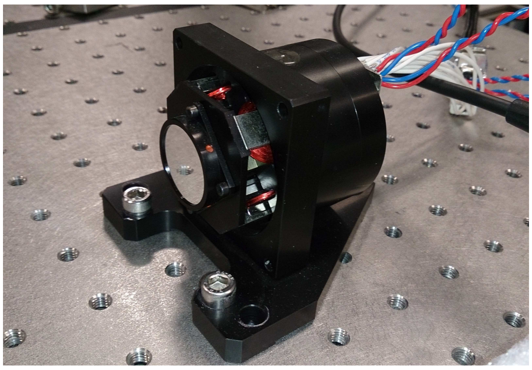

Fig. 1. Fast steering mirror system from Optics in Motion. The 1" mirror is actuated by two voice coils per axis and has a range of +/- 26.2 mrad. The coils are driven by external current amplifiers, with their input considered as system input. It has an internal optical sensor system for measuring the mirror position, which is considered as plant output.

I. INTRODUCTION

Fast steering mirrors (FSMs) have been available for several decades in the form of various electromagnetically [1], [2] and piezoelectrically [3], [4] actuated systems, which are typically operated with wide bandwidth (WBW) feedback controllers for fast motion control and disturbance rejection. Typical applications of FSMs are pointing and scanning of a laser or light beam [5], tracking of objects and acquisition of optical signals [6], and beam stabilization in optical systems [1]. With focus on exploiting the FSM's tip/tilt motion for scanning operations, applications span over a large range from laser scanners [2], over optical free space communication [3] to scanning optical lithography [7], scanning confocal microscopy [8], and to material processing [9].

As in other fields that apply 2-dimensional scanning of an area, e.g. in scanning probe microscopy (SPM) [10], raster scan trajectories are commonly employed scanning patterns [9], [11]. Systems with FSMs traverse the area of interest by deflecting a light beam by tilting the mirror around both axis (see Fig. 1). Each axis is driven with either a fast or a slow triangular signal, resulting in a uniform resolution and scan speed at every image location. Achieving high spatial resolution at high frame rates requires high system bandwidths, as at least the first 7 harmonics of the fundamental frequency should be covered [12]. This requires high bandwidth controllers [13] and imposes stringent requirements on the mechanical design of the FSM [14], in order not to excite unwanted structural modes of the system, as also known from e.g. nanopositioners [10]. Additionally the bandwidth of electromagnetically actuated FSMs is limited by the maximum actuator force, given by the maximum coil current. Besides the maximum scan frequency, limited by the system bandwidth, the application of raster scan patterns to a feedback controlled system without advanced control strategies leads to significant tracking errors, as known from other scanning systems [10]. This represents a challenge for high speed scanning applications that employ FSMs for tracking of a reference with high precision.

A possibility to improve the tracking behavior of scanning systems, is to employ Lissajous-based scan trajectories [15]. For systems with two orthogonal axes they result from driving each axis with a sinusoidal signal of a single frequency, with the frequencies determining the shape and the spatial resolution of the trajectory. Fig.2 shows a comparison of a Lissajous and a raster scan trajectory with equal resolution and frame rate.

Their use for scanning operations has been studied in different scientific applications like medical imaging [16] or optical microscopy [17]. Applicability of Lissajous scan trajectories for SPM systems and their multi-resolution capabilities have been demonstrated [15] and are applied to video-rate atomic force microscope (AFM) [18].

This paper introduces Lissajous trajectories for scanning operations of electromagnetically actuated low stiffness FSMs, aiming to improve the tracking performance of the system when compared to a raster scan. In Section II the experimental system is described and a system identification

[1]Authors are with the Christian Doppler Laboratory for Precision Engineering for Automated In-Line Metrology
[2]Automation and Control Institute Vienna University of Technology, 1040 Vienna, Austria. Corresponding author: csencsics@acin.tuwien.ac.at

Post-print version of the article: Ernst Csencsics, Rudolf Saathof and Georg Schitter, "Design of a dual-tone controller for Lissajous-based scanning of fast steering mirrors," *2016 American Control Conference (ACC)*, pp. 461-466, 2016. DOI: 10.1109/ACC.2016.7524957

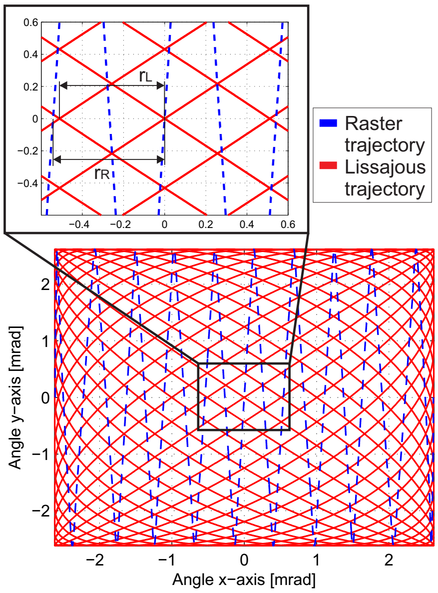

Fig. 2. Raster trajectory compared to Lissajous trajectory for a FSM tip/tilt system with scan size of 5.24 x 5.24 mrad (equals 10% of the used FSM system range) and scan speed of 1 frame/s. The fast axis of the raster scan is set to 10 Hz (70 Hz bandwidth required) and the Lissajous frequencies are set to f_x=19 Hz and f_y=14 Hz resulting in an almost equal spatial resolution r_R for the raster and r_L for the Lissajous scan (zoomed image).

for the commercial FSM test system is performed. To tailor a controller design to the narrow-band frequency spectrum of the drive signals and to deal with the low stiffness system properties, dual tone (DT) controllers with highly localized control efforts only at the drive frequencies are designed using an H$_\infty$-approach in Section III. The tracking performance of the FSM system with conventional WBW controllers and the tailored DT controller solutions are compared in Section IV by applying raster scan and Lissajous scan trajectories. In this course the tracking error and the energy consumption are evaluated.

II. SYSTEM DESCRIPTION AND IDENTIFICATION

To investigate the Lissajous and raster trajectories a commercial FSM (Type: OIM101, Optics in Motion LLC, Long Beach, USA) with a maximum range of +/-26.2 mrad (+/- 1.5 deg) is used (see Fig. 1). An internal optical sensor system with read-out electronics is used for measuring the mirror position and closed loop operation. Each axis is actuated by two voice coil actuators of the moving magnet type, which are operated in push-pull configuration. To be able to implement arbitrary controller designs the actuator coils of each axis are directly driven by a custom made current amplifier (OPA544T, Texas Instruments Inc., Dallas, TX, USA) with a bandwidth of 10 kHz. The controller implementation is done on a dSpace platform (Type: DS1202, dSPACE GmbH, Germany). The actuator and sensor axis of the FSM are 45° rotated with respect to each other. To decouple both axes and arrive at two single input single output (SISO) sub-systems, the dSpace system is also used to implement a rotation matrix for transforming the drive signals.

For system identification a system analyzer (3562A, Hewlett-Packard, Palo Alto, CA, USA) is used. The mirror, the amplifier and the internal sensor are together considered as the plant. The input of the power amplifier is considered as the system input and the signal of the internal sensor represents the system output. Due to the symmetric system design, the measured transfer functions (TFs) of both mirror axes are identical, as shown in Fig. 3. The cross-coupling between the axes is more than 42 dB lower (data not shown) than the single axis TFs (see Fig. 3) at DC and over most part of the relevant frequency range, which justifies the application of SISO controllers for each axis.

To model the measured frequency responses a second order plant model

$$P(s) = K \cdot \frac{\omega_0^2}{s^2 + 2\omega_0\zeta s + \omega_0^2} \cdot PA(s), \tag{1}$$

with a DC gain K=11.22, a 1st resonance frequency at 27 Hz (ω_0=169.6 rad/s) and a damping ratio ζ=0.04 is fitted. $PA(s)$ is a second order Pade-approximation [19] that is used to model the phase loss due to sampling at T_s=50 μs of the digital system in the frequency range below 2 kHz for the controller design.

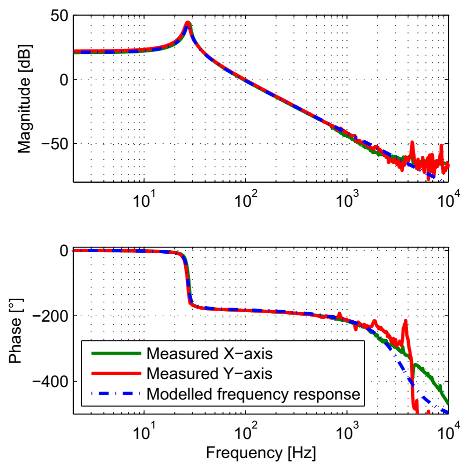

Fig. 3. Frequency responses of the FSM x- (solid green) and y-axis (solid red) measured with internal sensors and fitted system model (dashed blue). It is modeled as a mass-spring-damper system with a resonance frequency f_0=27 Hz and a damping ratio ζ=0.04. The 1st structural resonance occurs at 4 kHz. The time delay is caused by the sampling of the digital system at T_s=50 μs and is modeled by a 2nd order Pade approximation with a phase lag around 3.5 kHz.

Measurements with a capacitive sensor (Type: 6504, MicroSense LLC, Lowell, MA, USA) revealed structural modes of the mirror carrier above 800 Hz (data not shown), which are not observed with the internal sensors (see Fig. 3). Considering a precise scanning motion these unobservable dynamics would lead to deviations of the steered beam that

Post-print version of the article: Ernst Csencsics, Rudolf Saathof and Georg Schitter, "Design of a dual-tone controller for Lissajous-based scanning of fast steering mirrors," *2016 American Control Conference (ACC)*, pp. 461-466, 2016. DOI: 10.1109/ACC.2016.7524957

cannot be compensated and are thus limiting the maximum drive frequency of the mirror to below 800 Hz (i. e. the first unobservable mode).

All measurements are done on an optical table with a transmissibility of less than 0.01 for frequencies beyond 10 Hz. For the raster trajectory a signal composed of the first 7 harmonics of the fundamental frequency is considered for the input reference of the fast axis. As the system bandwidth is limited to below 800 Hz the fast axis frequency is set to $f_{R,f}$=100 Hz. The reference signal for the slow axis has a fundamental frequency of $f_{R,s}$=0.5 Hz (1 frame/s) and is composed of frequencies up to the 11th harmonic. This results in scan rate of 1 frame/s and a resolution relative to size of scan area of r_R=0.01.

For investigation of a Lissajous scan pattern a trajectory with equal spatial resolution, i.e. the largest distance between 2 intersections of the trajectory with a principle axis (see Fig. 2), is used. The two drive frequencies $f_{L,f}$=215 Hz and $f_{L,s}$=152 Hz are determined using the definition above [15], resulting in a spatial resolution relative to the scan area size of r_L=0.01 and a trajectory duration of T=1 s (1 frame/s).

Experiments are performed at the maximum scan amplitude for the combination of controller and scan trajectory, which is limited by the maximum coil current. The measured signals are post-processed by low-pass filters for reducing high frequency noise.

III. CONTROLLER DESIGN

A. Wide bandwidth controller design

As most commercial FSM systems are controlled by PID controllers, a PID controller structure is chosen as benchmark WBW controller for each axis. A classical PID approach for such systems is a reasonable choice, as the main plant dynamics is determined by the mass line in the range between 400 Hz and 2 kHz. The maximum frequency must be below 800 Hz in order to not excite structural modes of the mirror (see Section II). A controller is designed according to [20] such that the closed loop system has a control bandwidth of about 700 Hz. The PID controller shows integrative behavior with high gains at low frequencies in order to remove the steady state error in the closed loop system. The P-gain lifts the loop gain such that the mass line intersects the 0 dB line at the targeted cross-over frequency. The D-gain is chosen such that the phase lead reaches its maximum at the cross-over frequency to maximize the phase margin. A realization term stops the differential action at higher frequencies to limit the control effort at higher frequencies. This results in a second order controller of the form

$$C_{PID} = K_{PID} \cdot \frac{s^2 + 2\zeta_z \omega_z s + \omega_z^2}{s \cdot (s + \omega_p)}, \tag{2}$$

with K_{PID}=109.72, ω_p=2π1.65e3, ω_z=2π87 and ζ_z=0.896, which is shown by the dashed line in Fig. 6. The integration action is stopped around 50 Hz such that the phase recovers until the cross-over frequency at 500 Hz. The differential action enforces a controller phase lead of 55° at 500 Hz. The realization term shows a pole at ω_p, stopping the differential action at 1.65 kHz.

B. Dual tone controller design

In contrast to a raster trajectory, a Lissajous trajectory results from driving each axis with a single sinusoidal waveform of fixed frequency. It is thus possible to shape each SISO controller to a single tone (ST), so that their control effort is localized at the drive frequency of the individual axis [15]. Even though cross-talk between the axes is almost neglectable, it introduces additional small movement with the drive frequency of the other axis, respectively. This leads to periodic tracking errors that cannot be canceled by a ST controller. The simulated power spectral density (PSD) of the resulting tracking error for the fast axis of the FSM system with a ST controller, tracking a Lissajous trajectory with $f_{L,s}$ and $f_{L,f}$ (152 and 215 Hz) is normalized (to the largest PSD value with the ST controller) and shown in Fig. 4a. It reveals major periodic error components at the slower axis drive frequency of 152 Hz. The PSDs for the second axis show similar results at the respectively other frequency. For canceling these disturbances from the respectively other axis, a DT controller that shows localized high control efforts at both drive frequencies is needed.

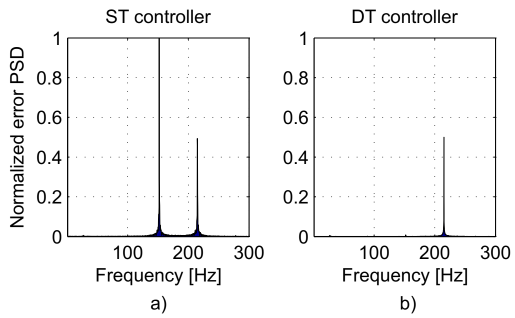

Fig. 4. Comparison of simulated normalized (to the largest value with the ST controller) PSDs of the resulting tracking error on the fast scanning axis (215 Hz) using (a) a ST and (b) the DT controller. The System tracks a Lissajous trajectory with drive frequencies 152/215 Hz. It can be seen that the periodical error at 152 Hz when using the ST controller can be entirely removed with the DT controller. The remaining error at 215 Hz results from deviations at the maximum values of the driving sine signal.

For tuning the DT controller a H_∞ design approach [19] is proposed, which allows to shape the sensitivity function S and the input sensitivity function U of the resulting system by weighting functions. The controller is obtained by minimizing the H-norm of the used extended model of a single axis (see Fig. 5) [21]. In Fig. 5, P represents the plant dynamics of the mirror, the amplifier, and the sensor, and C represents the controller. W_S and W_U are the weighting functions for the sensitivity function and the input sensitivity function, respectively, that are used to guide the controller design. p represents the sensed mirror position, r is the reference, e the resulting error, u the control effort and n the measurement noise.

The weighting function W_S, representing the requirements on S, is defined by a combination of two second-order

Post-print version of the article: Ernst Csencsics, Rudolf Saathof and Georg Schitter, “Design of a dual-tone controller for Lissajous-based scanning of fast steering mirrors,” *2016 American Control Conference (ACC)*, pp. 461-466, 2016. DOI: 10.1109/ACC.2016.7524957

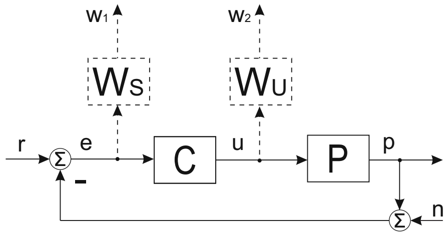

Fig. 5. Block diagram of the extended model for the derivation of a DT controller for one system axis. W_S and W_U are the weighting functions for the sensitivity function and the input sensitivity function, respectively. They are used to shape the controller C for tracking at a single drive frequency f_1 and rejecting the drive frequency f_2 of the second axis.

transfer functions

$$W_S(s) = \frac{s^2+2\omega_{r1}\zeta s+\omega_{r1}^2}{s^2+2\omega_{r1}\frac{\zeta}{d}s+\omega_{r1}^2} \cdot \frac{s^2+2\omega_{r2}\zeta s+\omega_{r2}^2}{s^2+2\omega_{r2}\frac{\zeta}{d}s+\omega_{r2}^2}. \quad (3)$$

Each second order transfer function represents an inverse notch filter and enforces low error sensitivity, thus good tracking, at one of the two drive frequencies. It reaches the peak exactly at the drive frequency and rolls off steeply before and after it, reducing the control effort at all other frequencies. The peak frequencies are determined for the chosen drive frequencies by ω_{r1}=955 rad/s ($f_{L,s}$) and ω_{r2}=1350.9 rad/s ($f_{L,f}$). Width and height of the inverse peak are tuned by the damping ratio ζ (0.01) and the factor d (100), respectively. To enforce a reduced control effort at higher frequencies the requirement on U is formulated by the weighting function

$$W_U(s) = 10 \cdot \frac{s+z_u}{s+p_u}, \quad (4)$$

with z_u=2π·2e2 and p_u=2π·2e6, which leads to a low pass behavior of the resulting system at higher frequencies. Given the system model presented in Section II and the weighting functions, the derived controller is of 8th order:

$$C_{H_\infty}(s) = K_{H_\infty} \cdot \frac{\left(\prod_{i=1}^{3} s^2+2\zeta_{z_i}\omega_{z_i}s+\omega_{z_i}^2\right)\cdot(s+\omega_{z_4})}{\prod_{i=1}^{4} s^2+2\zeta_{p_i}\omega_{p_i}s+\omega_{p_i}^2}, \quad (5)$$

with K_{H_∞}=1.303e5 and coefficients according to Table I. Fig. 4b shows that with the DT controller the error component at 152 Hz can entirely be removed. The remaining error at 215 Hz results from deviations at the maximum values of the driving sine signal. Besides improved tracking behavior at the drive frequencies, the controller also reduces sensor noise feedback from input n (see Fig.5) to the output of the system [15].

C. Controller implementation

Both continuous controllers are discretized using *Pole-Zero-Matching* [22] for a sampling frequency f_s=20 kHz. Poles an zeros are directly transformed to the discrete time domain using the relation $z = e^{s/f_s}$, ensuring that the DT

TABLE I
COEFFICIENTS OF THE DESIGNED H$_\infty$ DUAL TONE CONTROLLER.

Index	ω_{Index} [rad/s]	ζ_{Index}
z_1	170	4e-2
z_2	1140	-3e-3
z_3	22200	0.5
z_4	-148	N.A.
p_1	955	1e-4
p_2	1350	1e-4
p_3	20900	0.16
p_4	32900	0.75

controller poles are located exactly at the drive frequencies. The measured controller TF of the WBW and the DT controller are depicted in Fig. 6, showing significantly higher control gains of the DT controller at the Lissajous driving frequencies, while showing lower gains at all other frequencies as compared to the WBW controller.

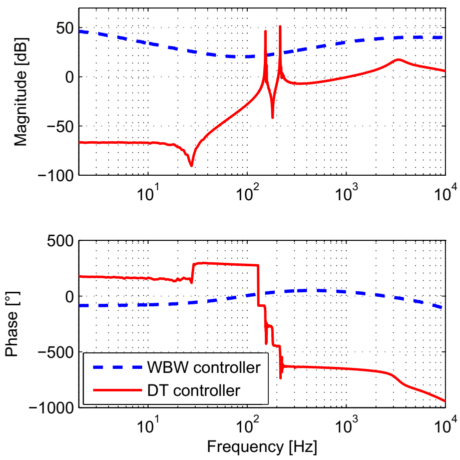

Fig. 6. Measured frequency response of the implemented WBW (dashed blue) and DT (solid red) controller. The WBW controller is a PID controller designed for a closed loop bandwidth of 700 Hz. The DT controller shows highly localized control efforts at the scan frequencies of 152 Hz and 215 Hz.

The measured complementary sensitivity functions for reference tracking of the resulting feedback controlled system are depicted in Fig. 7. The system with the WBW controller has a control bandwidth of about 730 Hz. The controller is thus suitable for the aimed raster scan fast axis frequency of 100 Hz, with the first 7 harmonics covered. From Fig. 7 it can be seen that the designed controller can also be used for Lissajous scan patterns with drive frequencies up to the control bandwidth. It, however, also indicates that increasing mismatches in phase and gain (slightly peaking before the roll-off), as a consequence of the PID design, may result in a rather poor tracking performance for higher drive frequencies.

The TF of the DT controller in Fig. 6 shows peaks of more than 45 dB at the drive frequencies, due to the chosen

W_S, while having the shape of the inverse system model at low frequencies with gains smaller than -50 dB below 50 Hz. Above 3 kHz the controller gain declines as a result of the chosen W_U. Fig. 7 shows that the closed loop TF with the DT controller reaches the 0 dB line exactly at the two drive frequencies, while remaining below -40 dB at lower and higher frequency ranges. Employing a right half plane zero at 177 Hz enforces also a perfect phase match of 360° and 720° at the drive frequencies (see Fig. 7). This phase match is achieved at the cost of a positioning delay of 1 and 2 sampling periods, respectively, depending on the drive frequency of the axis. The DT controller thus appears to be well suited for Lissajous trajectories. In contrast, a raster trajectory containing multiple frequency components that do not match the two designed DT frequencies can not be tracked. As the designed controller is tuned to both drive frequencies and the system is built symmetrically, the same controller can be used for both scan axes.

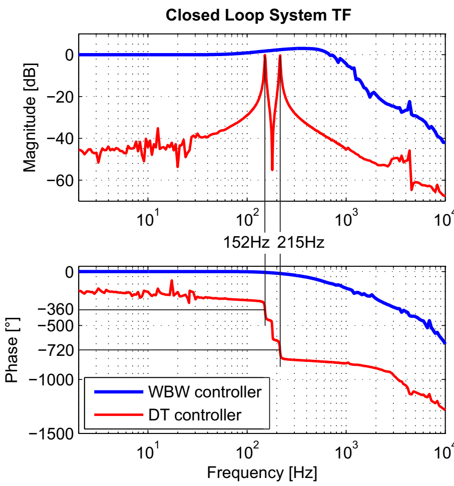

Fig. 7. Measured closed loop frequency response of the system with the WBW (blue) and the DT (red) controller. The control bandwidth with the WBW controller is 730 Hz. With the DT controller the transfer function reaches 0 dB at the drive frequencies (152/215 Hz) and lies below -35 dB for lower and higher frequency ranges.

IV. Experimental Results

The tracking performance of the system with WBW and DT controller is evaluated for both types of scan trajectories. Both controllers are evaluated for amplitudes of 8% (2.1 mrad) and 1% (0.26 mrad) of the full scan range. The WBW controller is applied for the raster scan at 100 Hz and for the Lissajous scan, while the DT controller is evaluated for the Lissajous scan only. Combinations of trajectories and controllers investigated are numbered from *E1* to *E5* and summarized in Table II. The results in tracking error and energy consumption are depicted in Fig. 9.

A. Wide bandwidth controller (E1 - E3)

Applying the raster pattern to the WBW controlled system, the output signal shows significant tracking errors at the turning points of the triangle as known from other scanning systems [10]. The system fast axis for a 100 Hz triangular reference with 2.1 mrad amplitude shows a maximum tracking error of 0.34 mrad (equals 16% of the amplitude). The RMS tracking error relative to the scan amplitude remains for both cases (*E1*, *E2*) around 9.2% (see Table II).

TABLE II
Investigated combinations of trajectories (equal relative spatial resolution of 0.01), controllers and scan amplitudes.

Nr.	Trajectory	Controller	Frequency [Hz]	Amplitude [mrad]
E1	Raster	WBW	100/0.5	0.26
E2	Raster	WBW	100/0.5	2.1
E3	Lissajous	WBW	215/152	2.1
E4	Lissajous	DT	215/152	2.1
E5	Lissajous	DT	215/152	0.26

The bandwidth of the WBW controller covers the drive frequencies of the Lissajous trajectory (see Section III-C). Applying the Lissajous trajectory (*E3*), however, reveals major RMS tracking errors of more than 37%. The main cause for the large periodic error is the increasing phase mismatch of the closed loop TF for higher frequencies (−18° at 215 Hz), while the gain mismatch (see Fig. 7) may play a minor role in this case. The line scan frequency (main component) of the raster trajectory lies at 100 Hz, where the TF is still unity, explaining the smaller error in the raster scanning case.

B. Dual tone controller (E4 - E5)

Fig. 8a shows the good tracking performance of the system for a measured Lissajous scan with 2.1 mrad amplitude (*E4*) in a zoomed area of 0.4x0.4 mrad around the center point. Fig. 8b, depicting the normalized (to the largest experimental

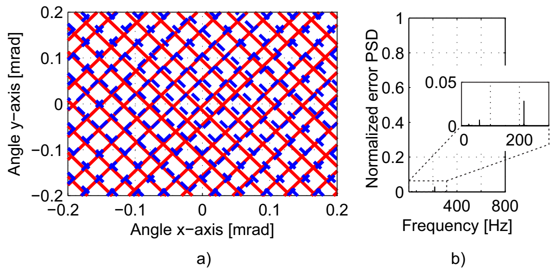

Fig. 8. Measured Lissajous scan with DT controller (*E4*). (a) shows the measured Lissajous trajectory (solid red) and the reference trajectory (dashed blue) for a scan amplitude of 2.1 mrad in a zoomed area of 0.4x0.4 mrad around the center point. Good tracking of the reference with only slight deviations is observed. (b) shows the PSD of the tracking error of the system fast axis normalized to the largest experimental error value from case (*E3*). A remaining small error component at 215 Hz is observable, resulting from deviations around the max. values of the driving sine wave. The component at 152 Hz is rejected.

error value from (*E3*)) PSD of the tracking error of the fast axis, indicates that the error is smallest for the Lissajous trajectory with the DT controller and that the frequency component of the slow axis (152 Hz) can be entirely rejected.

Post-print version of the article: Ernst Csencsics, Rudolf Saathof and Georg Schitter, "Design of a dual-tone controller for Lissajous-based scanning of fast steering mirrors," *2016 American Control Conference (ACC)*, pp. 461-466, 2016. DOI: 10.1109/ACC.2016.7524957

Comparing the Lissajous scan with the DT controller (*E4*) and the Lissajous scan with the WBW controller (*E3*) shows a significantly smaller RMS tracking error of only 0.77%. The remaining maximum tracking error is reduced to 0.03 mrad (equals 1.1% of the amplitude). Also the RMS current drops from 2.69 A to 1.99 A, showing a reduced energy consumption with the tailored controller. The resulting tracking error of the Lissajous scan with the DT controller is also significantly smaller than the raster scan with the WBW controller (*E2*) which is around 9.2%. Similar results are obtained for the small scan amplitude. The RMS current, however, is up to a factor 2.3 higher for the same scan amplitudes.

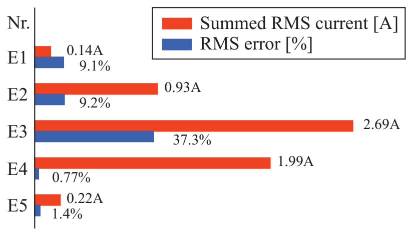

Fig. 9. Comparison of fast axis tracking error and energy consumption for the combinations specified in Table II. The summed RMS current of both actuation axes is depicted in red, and the RMS tracking error relative to the size of the related scan area is shown in blue. The Lissajous pattern with related controller shows the smallest error values of 0.77%.

In summary, Lissajous-based scanning in combination with DT control significantly reduces the tracking error while maintaining the same spatial and temporal resolution as compared to a raster-based scan of the FSM.

V. CONCLUSION

In this paper Lissajous trajectories are introduced to improve the tracking performance of electromagnetically actuated, low stiffness FSM scanning systems. Exploiting the narrow frequency spectrum of the reference signal a tailored dual-tone feedback controller design with highly localized control efforts at the drive frequencies is presented and experimentally verified. It is demonstrated that the controller can be used to eliminate periodic errors in the position signal that result from remaining cross-talk between the system axes and that it significantly outperforms a classical PID controller driven with the same Lissajous trajectory. Applying the tailored controller with related Lissajous trajectories the RMS tracking error can be reduced to 0.77%, as compared to more than 9.1% when doing a conventional raster scan. The peak error gets reduced from 16% for the raster to 1.1% for the Lissajous scan.

ACKNOWLEDGMENT

We would like to thank Andreas Sinn from ACIN at Vienna University of Technology for his help with the amplifier electronics. The financial support by the Austrian Federal Ministry of Science, Research and Economy and the National Foundation for Research, Technology and Development is gratefully acknowledged.

REFERENCES

[1] D. J. Kluk, M. T. Boulet, and D. L. Trumper, A high-precision, two-axis steering mirror with moving iron actuator. Mechatronics, vol. 22, no. 3, pp. 257, 2012.
[2] M. Hafez, T.C. Sidler, R.P. Salathe, G.L.M. Jansen, and J.C. Compter, Design, simulations and experimental investigations of a compact single mirror tip/tilt laser scanner. Mechatronics, vol. 10, no. 7, pp. 741, 2000.
[3] H. Mokbel, W. Yuan, L. Qiong Ying, C. Guo Hua, and A. A. Roshdy, Research on the Mechanical Design of Two-Axis Fast Steering Mirror for Optical Beam Guidance. Proceedings of the 1st International Conference on Mechanical Engineering and Material Science, Atlantis Press, 2012.
[4] F. M. Tapos, D. J. Edinger, T. R. Hilby, M. S. Ni, B. C. Holmes, and D. M. Stubbs, High bandwidth fast steering mirror. Optics and Photonics, pp. 587707, 2005. International Society for Optics and Photonics.
[5] S. H. Xiang, P. Wang, S. H. Chen, X. Wu, D. Xiao and X. W. Zheng, The Research of a novel single mirror 2D laser scanner. International Symposium on Photoelectronic Detection and Imaging, pp. 73821A, 2009. International Society for Optics and Photonics.
[6] M. Guelman, A. Kogan, A. Livne, M. Orenstein, and H. Michalik, Acquisition and pointing control for inter-satellite laser communications. IEEE Transactions on Aerospace and Electronic Systems, vol. 40, nr. 4, pp. 1239, 2004.
[7] Q. Zhou, P. Ben-Tzvi, D. Fan, and A. Goldenberg, Design of Fast Steering Mirror systems for precision laser beams steering. International Workshop on Robotic and Sensors Environments, pp. 144, 2008. IEEE.
[8] H.W. Yoo, M. E. van Royen,W. A. van Cappellen, A. B. Houtsmuller, M. Verhaegen, and G. Schitter, Automated spherical aberration correction in scanning confocal microscopy. Review of Scientific Instruments, vol. 85, pp. 123706, 2014.
[9] L. R. Hedding and R. A. Lewis, Fast steering mirror design and performance for stabilization and single axis scanning. presented at International Society for Optics and Photonics Orlando '90, Orlando, FL, April 16-20, pp.14, 1990.
[10] G.Schitter, P.J. Thurner, and P. Hansma, Design and input-shaping control of a novel scanner for high-speed atomic force microscopy. Mechatronics, vol. 18, nr. 5, pp. 282, 2008.
[11] S. Xiang, S. Chen, X. Wu, D. Xiao, and X. Zheng, Study on fast linear scanning for a new laser scanner. Optics and LASER technology, vol. 41, nr. 1, pp.42, 2010.
[12] A. J. Flemming and A. G. Wills, Optimal periodic trajectories for band-limited systems. IEEE Transactions on Control Systems Technology, vol. 17, nr. 3, pp. 552, 2009.
[13] H. W. Yoo, S. Ito, and G. Schitter, Iterative Learning Control of a Galvanometer Scanner for Fast and Accurate Scanning Laser Microscopy. Control Engineering Practice, under review, 2015.
[14] M. N. Sweeney, G. A. Rynkowski, M. Ketabchi, and R. Crowley, Design considerations for fast-steering mirrors (FSMs). International Symposium on Optical Science and Technology, pp. 63, 2002. International Society for Optics and Photonics.
[15] T. Tuma, J. Lygeros, V. Kartik, A. Sebastian and A. Pantazi, High-speed multiresolution scanning probe microscopy based on Lissajous scan trajectories. Nanotechnology, vol. 23, no. 18, pp. 185501, 2012.
[16] H. Feng, H. Gu, D. Silbersweig, E. Stern, and Y. Yang, Single-shot MR imaging using trapezoidal-gradient-based Lissajous trajectories. IEEE Transactions on Medical Imaging, vol. 22, nr. 8, pp. 925, 2003.
[17] S. Z. Sullivan et al., High frame-rate multichannel beam-scanning microscopy based on Lissajous trajectories. Optics Express, vol. 22, nr. 20, pp. 24224, 2014.
[18] A Bazaei, Y. K. Yong and S. R. Moheimani, High-speed Lissajous-scan atomic force microscopy: Scan pattern planning and control design issues. Review of Scientific Instruments, vol. 83, nr. 6, pp. 063701, 2012.
[19] S. Skogestad and I. Postlethwaite, Multivariable Feedback Control. John Wiley, New York, 2005.
[20] R. Munnig Schmidt, G. Schitter, A. Rankers, and J. van Eijk, The Design of High Performance Mechatronics. Delft University Press, 2nd ed., 2014.
[21] H. Kwakernaak. Robust control and H∞-optimization - Tutorial Paper. Automatica, vol. 29, no. 2, pp. 255, 1993.
[22] G. F. Franklin, D. J. Powell and M. L. Workman, Digital Control of Dynamic Systems. Prentice Hall, 1997.

Post-print version of the article: Ernst Csencsics, Rudolf Saathof and Georg Schitter, "Design of a dual-tone controller for Lissajous-based scanning of fast steering mirrors," *2016 American Control Conference (ACC)*, pp. 461-466, 2016. DOI: 10.1109/ACC.2016.7524957